

# Two-Dimensional Anion Exchange coupling Size Exclusion Chromatography Combined with Mathematical Modeling for Downstream Processing of Foot and Mouth Diseases Vaccine

Alireza Ghassempour<sup>1</sup>, Seyed Mohammad Javad Hossienizadeh<sup>2</sup>, Mohsen Bagheri<sup>2</sup>, Mahdi Alizadeh<sup>2</sup>, Masoud Rahimi<sup>2</sup>, Mahmoud Azimi<sup>3</sup>, Morteza Kamalzade<sup>3</sup>, and Ali Es-haghi<sup>3</sup>

<sup>1</sup>Department of Phytochemistry,

<sup>2</sup>Shahid Beheshti University

<sup>3</sup>Razi Vaccine & Serum Research Institute

September 11, 2020

## Abstract

The production of purified virus particles with high quality and quantity for vaccine preparation requires scalable purification procedure in downstream step. A purification scheme based on combined strong anion-exchange and size exclusion chromatography (2D -AEC×SEC) is developed for production non-structural protein (NSP) free foot and mouth diseases (FMD) vaccine and the whole procedure is accomplished with 78 % recovery, 85 % virus yield and more than 90 % of residual DNA (rDNA) is removed from the purified vaccine. Due to use AEC as the first column, the injection volume increases four times compare to previous report. Alternatively, a mathematical modeling and simulation approach based on plate model chromatography are developed and matched with the experimental chromatography data to obtain better perception in predicting retention behavior and saving time in downstream scale-up method development. The analysis of purified virus particles by sodium dodecyl sulfate-polyacrylamide gel electrophoresis (SDS-PAGE), dynamic light scattering (DLS) high performance size exclusion chromatography (HP-SEC), matrix-assisted laser desorption/ionization time-of-flight mass spectrometry (MALDI-TOF MS), transmission electron microscopy (TEM) and biological test provide to the best quality of purified FMD virus.

## 1. Introduction

From biopharmaceutical point of view, the downstream procedures becoming a critical bottleneck, which usually requires up to 80% of the overall construction cost of a protein product (Kol et al., 2020). Foot and mouth disease (FMD) is a severe and acute systemic viral vesicular trans-boundary disease of cloven-hoofed animals such as cattle, pigs, and sheep with a remarkable economic impact (Kleid et al., 1981; MacDonald, 2018). The etiological agent of FMD is foot-and-mouth disease virus (FMDV), which belongs to the genus *Aphthovirus* in the family of *Picornaviridae* (Azeem et al., 2020). FMDV particles consist of a non-enveloped icosahedral capsid with a single-stranded positive-sense RNA genome of approximately 8,500 nucleotide which is surrounded by four structural proteins (VP<sub>1-4</sub>). The FMDV particle is roughly spherical in shape and about 25–30 nm in diameter (Domingo et al., 2002; Grubman & Baxt, 2004; MacDonald, 2018). The current FMD vaccines are produced in a multi-step procedure by replicating the virulent FMDV in baby hamster kidney cell lines (BHK) and is formulated with different adjuvants after inactivating with binary ethylenimine (BEI) chemically (Hassan, 2016; S.-Y. Lee et al., 2017). However, there are a number of concerns with this type of vaccines due to different amounts of critical impurities such as viral non-structural proteins (NSPs) and residual DNA (rDNA) of host cell. The existence of NSPs in vaccinated animals develop antibody responses in addition to the active ingredient of vaccine against these contaminate proteins, false positive differentiation infected from vaccinated animals, and rDNA leading to some unintended adverse effects in susceptible animals

or human consumers (Lee, et al. 2006). The traditional approaches used for purifying and concentrating FMD vaccine are based on ultracentrifugation on sucrose or CsCl gradient (Lee et al., 2020; Yamamoto et al., 1988), and salting out with anti-chaotropic agents such as ammonium sulphate or polyethylene glycol precipitation (Ferreira, et al. 2000; Gavier-Widen et al., 2012; Kim et al., 2019; Kleid et al., 1981; Lee et al., 2006). These processes cannot meet the aforementioned requirements since they are usually time-consuming, difficult to scale up, and affect biological activities considerably. Membrane ultrafiltration (UF) could not produce a high quality for the final vaccine product although it has been used for concentration, buffer exchange, and partial purification of FMD vaccine (Kim et al., 2019). Various chromatographic techniques have shown a growing trend in downstream process of vaccine and proteins purification (Heath et al., 2018; Santry et al., 2020; Tseng et al., 2018; Valkama et al., 2020; Wang et al., 2019). In general, FMDV particles have been purified using standard and scalable chromatographic techniques which separate them based on different properties such as biorecognition or ligand specificity, like affinity chromatography (Kramberger, et al. 2015; Rodrigues, et al. 1991; Zhao et al., 2019), isoelectric point (ion exchange chromatography, IEX) (Namatovu et al., 2013), surface hydrophobicity (hydrophobic interaction chromatography) (Giebel et al., 2010; Li et al., 2015; Namatovu et al., 2013), and size or hydrodynamic diameter (size exclusion chromatography) (Klein & Helfferich, 1970; Rhee & Amundson, 1982). The main drawback of SEC is related to low loading capacity, which is usually 0.5-4% total column volume in a group separation mode, and limits its application in the downstream of biopharmaceutical production (Chisti & Moo-Young, 1990). IEX is generally performed in the bind-elute mode instead of flow-through mode (target passes contaminant bind). Thus, most of the host cell protein (HCP) impurities are collected in the flow-through, while virus particles and some other impurities are absorbed on the ion-exchanger groups immobilized on surface media (Li et al., 2015). Anion or cation exchange resins have been used according to the  $pI$  of the active ingredient of proteins and vaccines (Benedini et al., 2020).

The performance of IEX can be accomplished mathematically with different models such as Plate Model and Rate Model to simulate elution curve, predict retention time, develop scale-up or process in various operational conditions, and reduce cost and time significantly during the process development (Benedini et al., 2020; Klein & Helfferich, 1970; Rhee & Amundson, 1982). For instance, Schmidt et al. (Schmidt et al., 2014), employed a stoichiometric displacement model in order to detect the retention behavior of a kind of protein at various pH gradient elution in a cation-exchange chromatography column. They also applied the model for studying the separation of an acid variant of the antibody. Benedini et al. (Benedini et al., 2020), developed a mathematical model to describe an anion exchange chromatography (AEC) column, which was expedient for purifying the real and unknown mixtures of proteins.

In our previous work, we applied two-dimensional SEC method assisted with mathematical modeling for purifying FMDV and investigation dynamic behavior of the SEC media towards FMDV active ingredient and some critical impurities such as NSPs and rDNA (Bagheri, et al., 2018; Helfferich & James, 1970). In the present study, a combination of AEC as the first column and SEC as the second column (2D - AEC×SEC) has been introduced to improve purifying the FMDV in larger sample size as well as in less period of time. In addition, 2D -AEC×SEC was accompanied with mathematical modeling in both dimensions for evaluation separation procedure to produce NSP free FMD vaccine. This new method significantly improves loading capacity and reduces time for FMDV purification. Finally, the purified virus particles were partially characterized by sodium dodecyl sulfate–polyacrylamide gel electrophoresis (SDS-PAGE), dynamic light scattering (DLS), high performance size exclusion chromatography (HP-SEC), Matrix-Assisted Laser Desorption/Ionization Time-of-Flight Mass Spectrometry (MALDI-TOF MS), and transmission electron microscopy (TEM).

## 2. Materials and Methods

### 2.1. Chemicals, media and solutions

All chemical and biochemical materials were in analytical grade, and buffer solutions were prepared using Milli-Q water (Millipore, USA). Then, bovine serum albumin ([?]99.5%, BSA, 66.4 kDa) and Blue dextran 2000 (2000 kDa) were purchased from Sigma-Aldrich (St. Louis, MO, USA). In addition, potassium

chloride was obtained from Mojallali Co. (Tehran, Iran). Further, Tris (hydroxyl methyl) amino methane was purchased from Sinchem (Jiangsu, China). In the next procedure, SEC and IEX were conducted on chromatographic media Sup-200 and Q-Sepharose XL virus license, respectively. Finally, chromatography columns XK 16 and XK 26 and size exclusion/ ion-exchange media were purchased from GE Healthcare (Illinois, USA).

## 2.2. Instrumentation

A high pressure gradient *AZURA* Lab Bio LC system from Knauer (Berlin, Germany) equipped with a biocompatible buffer pump P 6.1L including two pump heads to perform a gradient between two buffers, a single wavelength UV detector 2.1L with a 5-mm optical path flow cell, a *AZURA* CM 2.1S conductivity monitor, and a multifunctional assistant module for sample injection, column switching, and fractionation collector was used for different experiments in this study. Clarity chrome software was used for instrument control, data acquisition and data processing. The purification steps were done by two XK 16 (16x400 mm, I.D) and XK 26 (26x600 mm, I.D) columns from GE Healthcare (Illinois, USA). XK 16 is packed with Q-Sepharose XL virus licensed as the first dimension and XK 26 is packed with Superdex 200 prep grade (Sup-200) as the second dimension. Chromatographic runs in the first dimension was performed based on anion exchange (flow rate 8 mL/min, mobile phase A including 20 mM Tris-HCl, pH 7.3, mobile phase B including 20 mM Tris-HCl, 500 mM KCl, pH 7.3), sample volume (120 mL by feed pump loading), and the second column as size exclusion (flow rate 2.5 mL/min, mobile phase 20 mM Tris-HCl, 150 mM NaCl, pH 7.3), and volume of injection (3 mL). The columns have circulating jacket and they maintained at 4 degC temperature by a cooling system and chromatograms were recorded at the wavelength of 280 nm. All buffers and samples were filtered through 0.45  $\mu$ m, Acrodisc<sup>®</sup> *Syringe Filters*, before starting the experiments. The sanitization of the columns were performed with 0.5 M sodium hydroxide for at least one column volume after experiments and equilibrated with loading buffer. Finally, the columns were stored in 20% (v/v) ethanol at the room temperature for long-time storage.

## 2.3. High performance size exclusion chromatography

High performance size exclusion chromatography (HP-SEC) was applied for evaluating the capability of 2D-AEC $\times$ SEC for production NSP-free FMD vaccine, as well as the most important factors affecting the quality of the final products, integrity of active ingredient of vaccine, by monitoring fingerprint HPLC elution profiles of the purified FMDV fractions throughout the purification procedure as describe before (Bagheri et al., 2018). Briefly, HP-SEC analysis was performed on a Knauer HPLC system equipped with a photodiode array detector (PDA) set up at 280 nm and controlled by EZChrom Elite software. The HPLC conditions included Ultrahydrogel Linear (300  $\times$  7.8 mm, I.D.) analytical column from Waters (NJ 07054, US), solvent system consisting of 50 mM phosphate buffer with pH 7.2 containing 100 mM Na<sub>2</sub>SO<sub>4</sub> as the mobile phase, the flow rate of 0.6 mL/min, and the injection volume of 100  $\mu$ l.

## 2.4. Inactivated virus

FMDV strain O<sub>2016</sub> was propagated in BHK-21 cell suspension cultures at industrial scale bioreactor, and finally inactivated by BEI. Then, cell debris were primarily removed by centrifuge at 4500 rpm in 20-min filtration through a 0.45  $\mu$ m membrane from Sartorius Stedim Biotech (Gottingen, Germany). Finally, the crude virus bulk was concentrated about 23-fold using a 100-kDa cut-off diafiltration membrane in a tangential flow filter cassette from Sartorius Stedim Biotech (Gottingen, Germany). The FMDV concentrate samples were originally obtained from Vaccine and Serum Research Razi Institute (Karaj, Iran) after the aforementioned cultivation and pretreatment procedure.

## 2.5. Infectivity assay

The viral titer was determined by 50% cell-culture-infective-dose (CCID<sub>50</sub>) of Reed and Muench approach. Briefly, the serial tenfold dilutions of a pooled virus fraction obtained from different purification step in Eagle's Minimum Essential Medium (pH=7.3) was inoculated for 48 h on IBRS2 monolayer cell culture prepared in 96-well micro plate and was incubated for 72 h after the inoculation. Virus infectivity was

calculated as describe before (Frenz & Horváth, 1985).

## 2.6. Transmission electron microscopy (TEM) analysis

The pooled virus fraction obtained from final polishing step of 2D-AEC×SEC was transferred to a 400 mesh copper grid, left to dry without any further treatment, and negatively stained with 1% uranyl acetate solution for 1 min. The grids were viewed using a Philips FEITecnai 20 transmission electron microscopy (TEM, Royal Philips Electronics, Amsterdam) transmission electron microscope.

## 2.7. Dynamic light scattering (DLS) analysis

The structural integrity of the purified virus particle, along with TEM analysis can be determined by the size distribution profile through dynamic light scattering (DLS) approach. The DLS studies were performed on Nanophox (Sympatec GmbH, Claushtal, Germany) in a buffer containing 20 mM Tris-HCl, pH 7.3 at the room temperature.

## 2.8. SDS-PAGE analysis

Purified fractions obtained from 2D-AEC×SEC were analyzed by 15% sodium dodecyl sulfate–polyacrylamide gel electrophoresis (SDS–PAGE) under the reduced condition. Briefly, virion particles were directly resuspended in SDS loading buffer, boiled at 100 °C for 10 minutes, and incubated at 55 °C for 2 h. The SDS-PAGE were set as 5% acrylamide/N,N bis-acrylamide for the stacking gel and 15% for the resolving gel, and a high range of pre-stained protein standards from Sinaclon Co. (Tehran, Iran) (MW 25–180 kDa) was used as the molecular weight marker. The gels were stained with Coomassie Brilliant Blue G-250 after electrophoresis to visualize the protein profiles on the polyacrylamide gel.

## 2.9. Protein extraction protocol and target plate preparation for MALDI-TOF MS analysis

The sample was prepared according to a short protein extraction protocol (Calderaro et al., 2014). The fractions obtained from 2D-AEC-SEC were treated as 30 µl of 70% formic acid from Merck co. (Darmstadt, Germany) in Mili-Q water / vigorous mixing, 30 µl pure acetonitrile from Merck co. (Darmstadt, Germany) /additional vigorous mixing, and finally centrifugation at 10,000 rpm for 5 minutes (Centrifuge 5415R, Eppendorf (Milano, Italy)). The purified FMDV was analyzed in a low (2–20 kD), medium (20–50 kD), and high (50–100 kD) molecular weight ranged by using MALDI TOF MS (Applied Biosystems 4800 MALDI-TOF/TOF) instrument. All of the samples were analyzed with MALDI TOF MS in a linear positive mode. Regarding the analysis in the low molecular weight range, equal volumes of supernatant were mixed with an equal volume of  $\alpha$ -cyano-4-hydroxycinnamic acid matrix solution in 50% acetonitrile containing 0.1% trifluoroacetic acid (TFA) from Merck co.( Darmstadt, Germany), spotted (0.7 µL) onto one pre-spotted Mass Standards Calibration Opti-TOF insert MALDI plate, air dried, and analyzed with a MALDI-TOF MS. As for the high molecular weight range, a saturated solution of synapinic acid (SA) was used as the matrix (50 mg/mL SA in 30:70 ACN: TFA 0.1% Merck co. (Darmstadt, Germany) and equal volumes of supernatant and matrix solution were mixed. Then, 0.7 µL of the prepared solution was spotted onto the same target plate as air-dried at the room temperature.

## 2.10. Mathematical Model

This section presents the general mass balance equations and their assumption used in simulating IEX processes. It is worth noting that the governing equations, parameters, and simulation procedure for SEC column modeling are in line with those in the previous study (Bagheri et al., 2018).

### 2.10.1. Governing equations

Some assumptions are introduced to derive the governing equations of the IEC theory (Gu, 2015; Yamamoto et al., 1983a, 1983b). 1. Plug flow with axial dispersion in the column. 2. Total and species material balances for the liquid phase. 3. Isothermal condition throughout the column. 4. The ion components are in dilute concentration, and then the effect of adsorption on the total mass balance is negligible. Thus, superficial velocity and volumetric flow rate remain constant. 5. Ideal mixing happens in the aqueous phase.

Further, the overall molar volume is constant according to the dilute concentration of ionic components. 6. Total exchange capacity of the resin inside the bed is constant. 7. Kinetic model was used to specify the overall mass transfer of ionic components between the bulk liquid and adsorbed phase. Additionally, the mass transfer should be overcome in mass transfer resistance within the boundary layer surrounding the particle, as well as mass transfer resistance within the resin particle. The second resistance usually controls the overall mass transfer rate. Therefore, a lumped mass transfer rate was employed along with solid-film resistance.

Generally, the model describing the IEX column includes material and momentum transport in the bulk liquid (mobile phase), mass transfer from the bulk liquid to the adsorbent (stationary phase), and mass transfer resistances which influence this transport.

### 2.10.2. General mass balance equation for IEX

The following equation is introduced for the general mass balance equation for describing the behavior of the exchanged counter-ion in the bulk liquid phase, i.e. each ionic species in the liquid phase enters into the ion-exchange column (Mehay & Gu, 2014).

$$-\varepsilon_i E_z \frac{\partial^2 c_b}{\partial z^2} + v_l \frac{\partial c_b}{\partial z} + \varepsilon_i \frac{\partial c_b}{\partial t} - (1 - \varepsilon_i) \sum_{\substack{k=1 \\ k \neq b}}^{nc} J_k = 0, \quad (1)$$

$c_b$  is the counter ion concentration in the liquid phase. In the above equations,  $E_z$  refers to the axial dispersion coefficient which can be calculated for each component as a function of the number of theoretical separation plates:

$$E_z = \frac{v_l H_B}{2 N_P \varepsilon_i}, \quad (2)$$

where  $v_l$ ,  $H_B$ ,  $N_P$ , and  $\varepsilon_i$  indicate the liquid velocity, column height, number of theoretical separation plates, and interparticle voidage, respectively.

It is worth noting that the axial dispersion (mixing) usually happens when a fluid flows through a packed column such as ion-exchangers (Gu, 2015).

In order to see where to include axial dispersion in the bed model, the dimensionless Peclet number is employed which quantifies the degree of the dispersion introduced into the system.

$$Pe = \frac{v_l H_B}{E_z}, \quad (3)$$

$Pe \sim 0$  indicates that the bulk liquid is well mixed leading to homogeneous liquid composition throughout the bed. For  $Pe < 30$ , the effect of axial dispersion on bed performance is significant, while the bed operates under near plug flow conditions for  $Pe > 100$ , and the bed operates under plug flow conditions for  $Pe \sim \infty$ .

In Eq. (1),  $J_k$  represents the mass transfer rate between the bulk liquid and resin. By considering the solid phase resistance in the film model assumption, mass transfer driving force for component  $k$  is expressed as a function of the solid phase loading as follows:

$$J_k = \frac{\partial w_k}{\partial t} = \text{MTC}_{sk} (w_k^* - w_k), \quad (4)$$

where  $\text{MTC}_{sk}$  shows the solid film mass transfer coefficient (MTC),  $w_k^*$  indicates the ion loading in equilibrium with liquid phase ion concentration ( $c_k$ ), and  $w_k$  is the ion loading on resin.

The Yamamoto isotherm (Yamamoto et al., 1988), which can successfully express the equilibrium of several combinations of protein and ion-exchange resin adsorbent, was employed in this regard.

$$\overline{w_k = (\alpha_{1k} + \beta_{2k}c_b^{\gamma_{3k}})c_k}, \quad (5)$$

where  $w_k$  is ion loading on resin,  $c_b$  shows counter ion concentration in liquid phase,  $c_k$  indicates ion concentration in liquid phase and  $\alpha_{1k}$ ,  $\beta_{2k}$  and  $\gamma_{3k}$  are considered as the isotherm parameters which are related to equilibrium constants, stoichiometric coefficient in mass action equilibrium, and possible changes in the ionic strength of the elution buffer.

Ultimately, in Eq. (1), the total charge of both liquid and resin must be kept neutral in which the number of counter-ions released from the resin and inflowing the liquid phase are determined by the amount of ions exchanged from the liquid phase (Ernest, Whitley, Ma, & Wang, 1997) as follows:

$$\overline{J_b = \sum_{\substack{k=1 \\ k \neq b}}^{nc} J_k}, \quad (6)$$

where  $J_b$  and  $J_k$  are counter ion material transfer rate and ion material transfer rate, respectively.

### 3. Results and Discussions

AEC with strong anion exchanger immobilized on the surface of the Sepharose and high sample loading capability is considered as a good candidate for acidic environmentally labile virus particles like FMDV, which can accomplish the most important criteria such as speed and capacity for capturing step. It can remove low FMDV loading limitation in the first column in 2D-SEC×SEC method (Bagheri et al., 2018). High resolution SEC fractionation media, in the second column, like Sup-200 as a final polishing step in combination with AEC in two-dimension configuration 2D-AEC×SEC should provide desirable resolution and selectivity for active ingredient of FMD vaccine and critical impurities, rDNA and NSPs. **Fig.1** represents a snapshot of the whole developed purification procedure. During the method development, mathematical modeling and simulation are applied in the first dimension for evaluating the reliability of elution pattern of FMDV particles, rDNA and bovine serum albumin (BSA) as a marker of NSPs, as well as in the second dimension based on the pervious study for providing more evidence in producing NSPs free vaccine products (Bagheri et al., 2018).

#### 3.1. Strong AEC for capturing step of FMDV vaccine purification

The art of keeping labile FMDV particles in their native conformation can guarantee the conservation of their structure and function throughout a chromatographic process. The sample loading is the most important bottleneck for application SEC in downstream step. Although, in our last work, application of 2D-SEC×SEC as an alternative strategy could compensate this drawback with increasing sample loading to 12.5% of total column volume but increase loadability to higher than, due to significant reduction of virus recovery in the first dimension, was impossible (Bagheri et al., 2018). In AEC step, selecting an appropriate pH is considered as one of the most important parameters so that the target protein can have the highest activity and opposite charge to bind to the ion exchangers. The application of cation exchange chromatography in acidic condition to bind target protein to media is impossible given that the highest infectivity and stability for FMDV particles was described in neutral pH (Liang et al., 2014), and early study indicated very close  $pI$  for FMDV particles to the BSA ( $pI=4.8$  (Rodrigues et al., 1991)) (data not shown). Thus, AEC can be considered as another alternative for keeping the protein structure of FMDV and compensating the low loading capacity of SEC in capturing step.

Diethylaminoethyl (DEAE) and quaternary ammonium (Q) ligands are regarded as two most common exploited anion exchange candidates. Comparison of DEAE and Q anion exchanger on Sepharose base

matrixes such as DEAE–Sephacrose Fast Flow and Q Sepharose Fast Flow revealed there are higher dynamic binding capacity for strong anion exchanger (Q) than weak anion exchanger (DEAE) (Helfferich & James, 1970). Therefore, in the prospective of sample loading capacity for capturing step Q anion exchanger seemed more suitable for downstream step of FMDV production, but the activity of the final product should be evaluated. Thus, the suitability of Q Sepharose XL in capturing FMDV purification was evaluated due to aforementioned advantages (**Fig. 1**).

### 3.2. 2D-AEC×SEC experimental operation conditions

Salt concentration, flow rate, pH, and sample volume are considered as the most important parameters which should be optimized for developing a proficient 2D-AEC×SEC methodology. Regarding the self-dissociation feature and highest immunity of FMDV particles reported at pH below 5.6 and also partially on neutral pH (Liang et al., 2014), the mean pH = 7.3 was selected at all of the optimization steps for the initial and elution buffers in both column dimensions.

As it was already mentioned, co-elution behavior of virus particles and BSA indicated that the  $pI$  values are very close together, and accordingly the selection of pH = 7.3 about three units higher than of the  $pI$  = 4.8 for BSA can guarantee absorption active ingredient of vaccine to ion-exchange media.

Regarding to theoretical concepts of IEX approach, sample should be loaded with the minimum ionic strength on the ion exchange media in order to prevent from competition between the ions in the medium and the target protein for adsorption on the ion exchanger. Therefore, 1.2 mS/cm, as the electrical conductivity of the initial buffer (Tri-HCl 20 mM with pH = 7.3) was considered as the reference in order to set the conductivity of primary feed stock. Based on an experimental study, a salt adjustment for the primary sample could provide a conductivity equivalent to 1.2 mS/cm as the initial buffer in AEC. In the elution step, potassium chloride (KCl) was used to adjust the ionic strength of the applied elution buffer. Accordingly, a buffer of Tris-HCl (20 mM with pH = 7.3) containing 500 mM KCl was used in a stepwise gradient mode for elution absorbed proteins with suitable conductivity.

Considering the Q-Sephacrose base media specifications, the mean flow rates of 3 mL/min and 8 mL/min were selected for loading and eluting steps the sample, respectively. In general, loading 20–30% of the total binding capacity of the column should provide the optimal resolution with gradient elution mode in IEC (Bailey & Tondeur, 1981). The total protein concentration of 0.473 mg/mL in the feed stock was determined by Bradford assay and performance of Q-Sephacrose matrix was evaluated for the sample volume in the range of 50-100 mL of the primary sample in combination with Sup-200 as the final polishing step. Then, the total fractions obtained from capturing step were analyzed by HP-SEC as our last work (Bagheri et al., 2018), and virus infectivity assay was determined by Reed and Muench’s method (Frenz & Horváth, 1985). **Fig. 2** represents the elution pattern of primary sample for minimum sample loading on Q-Sephacrose media and Sup-200. After analyzing the obtained fractions from the first dimension, the highest amount of FMDV particles was washed out from the column between 120-180 minutes for the sample loading which was two times more than the maximum loading in the previous study (Bagheri et al., 2018). Therefore, pooled virus fraction was concentrated by the concentration factor 10, and then 4 mL of this concentrated sample was loaded on the Sup-200. The comparison of elution pattern for 2D-AEC×SEC and 2D-SEC×SEC indicates a completely same elution pattern for both methods in the second dimension. Since the minimum sample volume loaded on the first dimension ( $V_{inj} = 50$  mL) is about two times more than the maximum loading capacity in SEC for 2D-SEC×SEC, it seems that AEC is considered as a better candidate for capturing step to fulfill speed and capacity as the two most important criteria in this step. Based on the obtained data, the overall purification time in the first dimension reduced by a factor of 0.7 in 2D-AEC×SEC than 2D-SEC×SEC. In order to ensure the efficiency of anion exchange media in the proposed three-step strategy, the volume of the sample loaded on the resin increased in different experiments to maximum 100 mL (equal to four times of the related amount in 2D-SEC×SEC (Bagheri et al., 2018).

**Fig. 3 (A)** and **(B)** represent the experimental data, as well as the simulation results of the elution pattern in the primary feed stock for maximum sample loading on a combination of Q-Sephacrose and Sup-200 media.

In the final polishing step for Sup-200, as the second dimension, the volumetric flow rate decreased to 2.5 mL/min for obtaining a better resolution between virus particles and NSPs marker, BSA, due to the higher concentration of the concentrated sample in an intermediate concentration step. The simulation results for retention behavior of BSA, virus, rDNA and IgG components in the first and second dimension were also depicted in **Fig. 3 (A)** and **(B)**. In AEC the coupled set of Equations. (1), (4), (5) and (6) incorporating plate model (Eq. 2, considering convection with dispersion based on plate number), was discretized and solved using finite element and orthogonal collocation techniques. It is worth mention that the number of theoretical plates was estimated experimentally from a pulse injection of acetone and following the UV chromatogram for determination peak width at half-height and retention time. Accordingly, the height of theoretical plate (HETP) was calculated as 0.01177 cm. In order to assess the effect of controlling diffusion versus convection mechanisms, Pe number, as an important parameter affecting the performance of separation process, was considered and estimated by Eq. (3). Therefore, for the total height of the bed  $H_B = 40$  cm, internal diameter of the bed column  $ID = 1.6$  cm and particle radius of adsorbent  $R_p = 45 - 165 \mu\mu$ , the optimum amount for flow rate (or Pe number) and eluents concentration for FMDV particles elution from Q-Sepharose media were studied by mathematical modeling to explore the most appropriate condition in AEC column. Acquire data demonstrated that a flow rate equal to 8 mL/min and a combination of 73% of buffer A (buffer without salt) and 27% of buffer B (buffer with 0.5 M salt concentration) can be applied as the most suitable operational condition to elute virus particles from Q-Sepharose in the first dimension. Accordingly, the concentration of KCl at the time of departure of the virus peak from AEC column was predicted equal to 0.129 M. This is nearly close to experimental data as indicated 0.135 M KCl concentration for FMDV elution from AEC column. Moreover, as illustrated in **Fig. 3 (A)**, simulation results in the first dimension demonstrated that peaks for virus, BSA and rDNA have interfering areas in the output of the AEC, which is satisfactory matched with experimental data. Same results for experimental and simulated investigations can be explained by very close  $I$  values for these components at natural pH. Similarly, mathematical modeling and simulation process was also applied for total bed height equal to  $H_B = 60$  cm, internal diameter of the bed column.  $ID = 2.6$  cm, particle radius of adsorbent  $R_p = 24 - 44 \mu\mu$  in the second dimension for prediction and obtaining optimal flow rate. Eventually a flow rate equal to 2.5 mL/min was obtained for optimized operation condition and achieved data in **Fig. 3 (B)** showed that the simulation results are well-matched with the experimental counterparts. Therefore, this model can be applied to scrutinize the scaling-up issue in term of geometry (enlarging the cross-section and length of the columns), flow rate and sample loading capacity in the columns.

### 3.3. Fingerprinting elution profile of FMDV in three stage purification strategy

In this study, according to previous reports (Martin & Synge, 1941; Rodrigues et al., 1991; Ruthven, 1984), HP-SEC on Ultra hydrogel linear analytical column was applied for comparing fingerprinting elution profiles in three stages of purification strategy (**Fig. 1**), and the output results are depicted in **Fig. 4**.

As shown in **Fig. 4**, significant differences are observed between elution profiles of primary sample (Solid line), intermediate concentration step (Dash line), and final polishing step (Dotted line) by moving from capturing step toward final polishing step. After the capturing step, most of the low molecular weight impurities like HCP and majority of rDNA were removed from pooled virus fraction. Considering, the elution profile of concentrated sample obtained from intermediate concentration step on Sup-200 (**Fig. 3B**), the perfect resolution between the signals related to virus particles and NSPs marker (BSA) can provide clear evidence for completely elimination of NSPs from final product. Accordingly, residual observed impurities in the purified virus fraction (**Fig. 4**) are probably related to negligible high molecular weight proteins like immunoglobulins. Furthermore, the elution profile of purified virus fraction obtained from polishing step demonstrated that final product has more than 85% purity.

**Fig. 5** displays SDS-PAGE result for confirming the identity of the purified FMDV product in the final polishing step. Electrophoresis process shows three bands related to  $VP_1$ ,  $VP_2$  and  $VP_3$  structural proteins between 25-35 kD while the fourth structural protein,  $VP_4$ , was removed from the gel for obtaining higher resolution between high molecular weight counterparts. Similar to the previous report, observed bands in

molecular weight higher than related amounts for virus structural proteins can be attributed to VP<sub>1</sub>-VP<sub>2</sub> dimer or VP<sub>3</sub>multimers (Harmsen, Jansen, Westra, & Coco-Martin, 2010).

### Characterization of purified FMDV

The size distribution profile and structure of purified FMDV particles were analyzed by DLS and TEM, **Fig. 6** , approaches in order to provide more evidence for preserving intact virus structure during purification procedure as the most important criteria in the development downstream processing. DLS analysis demonstrated a single peak with hydrodynamic diameter about 30 nm and image indicated that the most of the purified virus particles are spherical in shape and structurally intact. Therefore, the obtained results confirmed that the final product in 2D-AEC×SEC is qualified for production formulated FMD vaccine.

### MALDI-TOF MS analysis

Currently, high throughput technology like MALDI-TOF MS is becoming a common methodology in clinical microbiology or virus research and diagnostics labs (Amexis et al., 2001; Giebel et al., 2010; Ilina et al. 2005; Ruelle et al. 2004; Sjöholm et al. 2008; Soleimani et al. 2020). In this work for the first time application of MALDI-TOF MS for direct investigation of purified FMDV particles was explored and obtained results were compared with the previous report of application SELDI-TOF in FMDV study (Harmsen et al., 2010). Thus, the fractions obtained from 2D-AEC×SEC (purified virus) were analyzed by MALDI-TOF MS in low (2-20 kD) (**Fig. 6A** ), medium (20-50 kD) (**Fig. 6B** ), and high (50-100 kD) (**Fig. 6C** ) molecular weight. Regarding the low molecular weight, there is a high intense ion in  $m/z = 8.7138\text{kD}$  (**Fig. 6A** ), which is in line with the previous report related to myristoylated form of VP<sub>4</sub>, a structural protein did not appear on SDS-PAGE. In the medium molecular weight (**Fig. 6B** ), there is a low intense and a high intense ion in  $m/z = 24\text{ kD}$  and  $m/z = 27.9873\text{ kD}$ , respectively, which are probably correlated to the VP<sub>3</sub> and VP<sub>1</sub> structural proteins. As observed from **Fig. 6C** , in the high molecular weight, there is a low intense signal in  $m/z = 54.0321\text{ kD}$ , possibly corresponding to the dimer of VP<sub>1</sub>.

### 3.6. Performance of developed 2D-AEC×SEC for purification FMDV

Performance of the constructed *2D-AEC×SEC* approach was summarized in **Table 1** . In capturing step on Q-Sepharose virus licensed as first dimension about 89.8 recovery and 150-fold of purification were achieved. In addition, further purification led to 18-fold of purification with 92.20% recovery on Sup-200 as the second dimension in the final polishing step. Further, the whole procedure was performed with 77.91 % recovery in the proposed scheme for the production of NSP free FMDV vaccine. According to the HP-SEC data, the purified pooled virus fraction has purity higher than 85.00 % in the polishing step. Interestingly, rDNA in the primary feed stock decreased from 81.30 ng to 8.01 ng. Thus, over 90.10% of host cell rDNA was removed from the final product.

## 4. Conclusion

In the present study, based on the previous report for the production of NSP free of FMD vaccine by combination 2D-SEC×SEC, we proposed a new platform by replacing SEC in the capturing step with strong anion exchange media in order to compensate low sample loading and achieve higher speed and capacity. Alternatively, mathematical modeling and simulation were applied to predict the retention behavior of active ingredient in vaccine and critical impurities such as rDNA or NSPs. Thus, the results confirmed:

- 1- Strong anion exchange chromatography in combination with high resolution SEC media such as Sup-200 has acceptable performance for production NSP free FMD vaccine from the perspective of purity and virus recovery, higher than 89.8 % and 77.91% respectively.
- 2- Capability of mathematical modeling and simulation as a complementary methodology to experimental data will provide a powerful approach to predict retention behavior of large biomolecules such as FMD and rDNA in complex chromatographic phenomena such as IEX for development downstream processing of biotherapeutic such as virus vaccine.
- 3- Analysis of purified FMDV by SDS-PAGE and HP-SEC confirmed the satisfactory purity for final product.

4- Application of MALDI-TOF mass spectrometry in direct analysis of FMDV particles provide more evidence regarding to purity and structural information of purified FMDV.

## 5. Authorship contribution

**S. M. J. Hossienizadeh** and **M. Bagheri** , Data curation, Formal analysis, Investigation, Methodology, Validation, Visualization, Graphical abstract design and Writing - original draft. **M. Alizadeh** : Laboratory experiments. **M. Rahimi** : Simulation process and Mathematical modeling. **M. Azimi** : Virus sample preparation and Virus Activity test. **M. Kamalzade** : Virus sample preparation. **A. Es-haghi** : Validation. **A. Ghassempour** : Conceptualization, Project management, Writing - review and Editing.

## 6. Declaration of interest statement

The authors declare that there is no conflict of interest.

## Reference

Amexis, G., Oeth, P., Abel, K., Ivshina, A., Pelloquin, F., Cantor, C. R., . . . Chumakov, K. (2001). Quantitative mutant analysis of viral quasispecies by chip-based matrix-assisted laser desorption/ionization time-of-flight mass spectrometry. *Proceedings of the National Academy of Sciences*, *98* (21), 12097-12102. doi:<https://doi.org/10.1073/pnas.211423298>

Azeem, A., Rashid, I., Hassan, M. M., Asad, M., Kaukab, G., Tehseen, A., & Aamir, S. (2020). A review on foot and mouth disease in dairy animals, etiology, pathogenesis and clinical findings. *Pure Applied Biology*, *9* (1), 821-832. doi: <http://dx.doi.org/10.19045/bspab.2020.90088>

Bagheri, M., Norouzi, H. R., Hossienizadeh, S. M. J., Es-haghi, A., & Ghassempour, A. (2018). Development and modeling of two-dimensional fast protein liquid chromatography for producing non-structural protein-free food-and-mouth diseases virus vaccine. *J. Chromatogr. B*, *1096* , 113-121. doi:<https://doi.org/10.1016/j.jchromb.2018.08.014>

Bailly, M., & Tondeur, D. (1981). Two-way chromatography: flow reversal in non-linear preparative liquid chromatography. *Chemical Engineering Science*, *36* (2), 455-469. doi:[https://doi.org/10.1016/0009-2509\(81\)85028-2](https://doi.org/10.1016/0009-2509(81)85028-2)

Benedini, L. J., Figueiredo, D., Cabrera-Crespo, J., Gonçalves, V. M., Silva, G. G., Campani, G., . . . Furlan, F. F. (2020). Modeling and simulation of anion exchange chromatography for purification of proteins in complex mixtures. *Journal of Chromatography A*, *1613* , 460685. doi:<https://doi.org/10.1016/j.chroma.2019.460685>

Calderaro, A., Arcangeletti, M.-C., Rodighiero, I., Buttrini, M., Gorrini, C., Motta, F., . . . De Conto, F. (2014). Matrix-assisted laser desorption/ionization time-of-flight (MALDI-TOF) mass spectrometry applied to virus identification. *J Scientific reports*, *4* (1), 1-10. doi:<https://doi.org/10.1038/srep06803>

Chisti, Y., & Moo-Young, M. (1990). Large scale protein separations: engineering aspects of chromatography. *J Biotechnology advances*, *8* (4), 699-708. doi:[https://doi.org/10.1016/0734-9750\(90\)91992-P](https://doi.org/10.1016/0734-9750(90)91992-P)

Domingo, E., Baranowski, E., Escarmis, C., & Sobrino, F. (2002). Foot-and-mouth disease virus. *J Comparative immunology, microbiology infectious diseases*, *25* (5-6), 297-308. doi:[https://doi.org/10.1016/S0147-9571\(02\)00027-9](https://doi.org/10.1016/S0147-9571(02)00027-9)

Ernest, M. V., Whitley, R. D., Ma, Z., & Wang, N.-H. L. (1997). Effects of mass action equilibria on fixed-bed multicomponent ion-exchange dynamics. *Industrial & engineering chemistry research*, *36* (1), 212-226. doi:<https://doi.org/10.1021/ie960167u>

Ferreira, G. N., Monteiro, G. A., Prazeres, D. M., & Cabral, J. M. (2000). Downstream processing of plasmid DNA for gene therapy and DNA vaccine applications. *J. Trends in biotechnology*, *18* (9), 380-388. doi:[https://doi.org/10.1016/S0167-7799\(00\)01475-X](https://doi.org/10.1016/S0167-7799(00)01475-X)

Frenz, J., & Horváth, C. (1985). High performance displacement chromatography: calculation and experimental verification of zone development. *J AIChE journal*, *31* (3), 400-409. doi:<https://doi.org/10.1002/aic.690310307>

Gavier-Widen, D., Meredith, A., & Duff, J. P. (2012). *Infectious Diseases of Wild Mammals and Birds in Europe* : Wiley.

Giebel, R., Worden, C., Rust, S., Kleinheinz, G., Robbins, M., & Sandrin, T. (2010). Microbial fingerprinting using matrix-assisted laser desorption ionization time-of-flight mass spectrometry (MALDI-TOF MS): applications and challenges. In *Advances in applied microbiology*(Vol. 71, pp. 149-184): Elsevier.

Grubman, M. J., & Baxt, B. (2004). Foot-and-mouth disease. *J Clinical microbiology reviews*, *17* (2), 465-493. doi:<https://doi.org/10.1128/CMR.17.2.465-493.2004>

Gu, T. (2015). *Mathematical Modeling and Scale-up of Liquid Chromatography: With Application Examples* : Springer.

Harmsen, M., Jansen, J., Westra, D., & Coco-Martin, J. (2010). Characterization of foot-and-mouth disease virus antigen by surface-enhanced laser desorption ionization-time of flight-mass spectrometry in aqueous and oil-emulsion formulations. *J. Vaccine*, *28* (19), 3363-3370. doi:<https://doi.org/10.1016/j.vaccine.2010.02.084>

Hassan, A. I. (2016). Effect of different culture systems on the production of foot and mouth disease trivalent vaccine. *J Veterinary World*, *9* (1), 32. doi: <https://doi.org/10.14202/vetworld.2016.32-37>

Heath, N., Grant, L., De Oliveira, T. M., Rowlinson, R., Osteikoetxea, X., Dekker, N., & Overman, R. (2018). Rapid isolation and enrichment of extracellular vesicle preparations using anion exchange chromatography. *J Scientific reports*, *8* (1), 1-12. doi:<https://doi.org/10.1038/s41598-018-24163-y>

Helferich, F., & James, D. (1970). An equilibrium theory for rare-earth separation by displacement development. *J Journal of Chromatography A*, *46* , 1-28. doi:[https://doi.org/10.1016/S0021-9673\(00\)83961-8](https://doi.org/10.1016/S0021-9673(00)83961-8)

Irina, E. N., Malakhova, M. V., Generozov, E. V., Nikolaev, E. N., & Govorun, V. M. (2005). Matrix-assisted laser desorption ionization-time of flight (mass spectrometry) for hepatitis C virus genotyping. *Journal of clinical microbiology*, *43* (6), 2810-2815. doi: <http://dx.doi.org/10.1128/JCM.43.6.2810-2815.2005>

Kim, H., Kim, A.-Y., Kim, J.-S., Lee, J.-M., Kwon, M., Bae, S., . . . Ko, Y.-J. (2019). Determination of the optimal method for the concentration and purification of 146S particles for foot-and-mouth disease vaccine production. *J. Virol. Methods*, *269* , 26-29. doi:<https://doi.org/10.1016/j.jviromet.2019.04.009>

Kleid, D. G., Yansura, D., Small, B., Dowbenko, D., Moore, D. M., Grubman, M. J., . . . Bachrach, H. L. (1981). Cloned viral protein vaccine for foot-and-mouth disease: responses in cattle and swine. *J. Science*, *214* (4525), 1125-1129. doi:<https://doi.org/10.1126/science.6272395>

Klein, G., & Helferich, F. G. (1970). *Multicomponent Chromatography: Theory of Interference* .

Kol, S., Ley, D., Wulff, T., Decker, M., Arnsdorf, J., Schoffelen, S., . . . Chiang, A. W. (2020). Multiplex secretome engineering enhances recombinant protein production and purity. *J Nature communications*, *11* (1), 1-10. doi:<https://doi.org/10.1038/s41467-020-15866-w>

Kramberger, P., Urbas, L., & Štrancar, A. (2015). Downstream processing and chromatography based analytical methods for production of vaccines, gene therapy vectors, and bacteriophages. *J Human vaccines immunotherapeutics*, *11* (4), 1010-1021. doi:<https://doi.org/10.1080/21645515.2015.1009817>

Lee, F., Jong, M.-H., & Yang, D.-W. (2006). Presence of antibodies to non-structural proteins of foot-and-mouth disease virus in repeatedly vaccinated cattle. *J Veterinary microbiology*, *115* (1-3), 14-20. doi:<https://doi.org/10.1016/j.vetmic.2005.12.017>

Lee, M. J., Jo, H., Park, S. H., Ko, M.-K., Kim, S.-M., Kim, B., & Park, J.-H. (2020). Advanced Foot-And-Mouth Disease Vaccine Platform for Stimulation of Simultaneous Cellular and Humoral Immune Responses. *J*

*Vaccines*, 8 (2), 254. doi:<https://doi.org/10.3390/vaccines8020254>

Lee, S.-Y., Lee, Y.-J., Kim, R.-H., Park, J.-N., Park, M.-E., Ko, M.-K., . . . Kim, S.-M. (2017). Rapid engineering of foot-and-mouth disease vaccine and challenge viruses. *Journal of Virology*, 91 (16). doi:<https://doi.org/10.1128/jvi.00155-17>

Li, H., Yang, Y., Zhang, Y., Zhang, S., Zhao, Q., Zhu, Y., . . . Su, Z. (2015). A hydrophobic interaction chromatography strategy for purification of inactivated foot-and-mouth disease virus. *Protein. Express. Purif.*, 113 , 23-29. doi:<https://doi.org/10.1016/j.pep.2015.04.011>

Liang, T., Yang, D., Liu, M., Sun, C., Wang, F., Wang, J., . . . Yu, L. (2014). Selection and characterization of an acid-resistant mutant of serotype O foot-and-mouth disease virus. *J Archives of virology*, 159 (4), 657-667. doi:<https://doi.org/10.1007/s00705-013-1872-7>

MacDonald, J. (2018). *Prospects of Plant-Based Vaccines in Veterinary Medicine* : Springer.

Martin, A., & Synge, R. M. (1941). A new form of chromatogram employing two liquid phases: A theory of chromatography. 2. Application to the micro-determination of the higher monoamino-acids in proteins. *J Biochemical Journal*, 35 (12), 1358. doi:<https://doi.org/10.1042/bj0351358>

Mehay, A., & Gu, T. (2014). A general rate model of ion-exchange chromatography for investigating ion-exchange behavior and scale-up. *J Microb Biochem Technol*, 6 , 216-222. doi:<https://doi.org/10.4172/1948-5948.1000147>

Namatovu, A., Wekesa, S. N., Tjørnehøj, K., Dhikusooka, M. T., Muwanika, V. B., Siegmund, H. R., & Ayebazibwe, C. (2013). Laboratory capacity for diagnosis of foot-and-mouth disease in Eastern Africa: implications for the progressive control pathway. *J BMC veterinary research*, 9 (1), 19. doi:<https://doi.org/10.1186/1746-6148-9-19>

Rhee, H. K., & Amundson, N. R. (1982). Analysis of multicomponent separation by displacement development. *J AIChE journal*, 28 (3), 423-433. doi:<https://doi.org/10.1002/aic.690280310>

Rodrigues, A., Dias, M., & Lopes, J. (1991). Theory of linear and nonlinear chromatography. In *Chromatographic and Membrane Processes in Biotechnology* (pp. 25-52): Springer.

Ruelle, V., Moulaj, B. E., Zorzi, W., Ledent, P., & Pauw, E. D. (2004). Rapid identification of environmental bacterial strains by matrix-assisted laser desorption/ionization time-of-flight mass spectrometry. *J Rapid Communications in Mass Spectrometry*, 18 (18), 2013-2019. doi:<https://doi.org/10.1002/rcm.1584>

Ruthven, D. M. (1984). *Principles of adsorption and adsorption processes* : John Wiley & Sons.

Santry, L. A., Jacquemart, R., Vandersluis, M., Zhao, M., Domm, J. M., McAusland, T. M., . . . Wootton, S. K. (2020). Interference chromatography: a novel approach to optimizing chromatographic selectivity and separation performance for virus purification. *J BMC biotechnology*, 20 (1), 1-15. doi:<https://doi.org/10.1186/s12896-020-00627-w>

Schmidt, M., Hafner, M., & Frech, C. (2014). Modeling of salt and pH gradient elution in ion-exchange chromatography. *Journal of separation science*, 37 (1-2), 5-13. doi:<https://doi.org/10.1002/jssc.201301007>

Sjoholm, M. I., Dillner, J., & Carlson, J. (2008). Multiplex detection of human herpesviruses from archival specimens by using matrix-assisted laser desorption ionization-time of flight mass spectrometry. *Journal of clinical microbiology*, 46 (2), 540-545. doi:<https://doi.org/10.1128/JCM.01565-07>

Soleimani Mashhadi, I., Shahmirzaie, M., Aliahmadi, A., Safarnejad, M. R., & Ghassempour, A. (2020). Conjugation of Single-Chain Variable Fragment Antibody to Magnetic Nanoparticles and Screening of Fig Mosaic Virus by MALDI TOF Mass Spectrometry. *J Analytical Chemistry* . doi:<https://doi.org/10.1021/acs.analchem.0c01119>

Tseng, Y.-F., Weng, T.-C., Lai, C.-C., Chen, P.-L., Lee, M.-S., & Hu, A. Y.-C. (2018). A fast and efficient purification platform for cell-based influenza viruses by flow-through chromatography. *J Vaccines*, *36* (22), 3146-3152. doi:<https://doi.org/10.1016/j.vaccine.2017.03.016>

Valkama, A. J., Oruettebarria, I., Lipponen, E. M., Leinonen, H. M., Kayhty, P., Hynynen, H., . . . Heikura, T. (2020). Development of large-scale downstream processing for lentiviral vectors. *J Molecular Therapy-Methods Clinical Development* . doi:<https://doi.org/10.1016/j.omtm.2020.03.025>

Wang, C., Mulagapati, S. H. R., Chen, Z., Du, J., Zhao, X., Xi, G., . . . Schmelzer, A. E. (2019). Developing an Anion Exchange Chromatography Assay for Determining Empty and Full Capsid Contents in AAV6. *J Molecular Therapy-Methods Clinical Development*, *15* , 257-263. doi:<https://doi.org/10.1016/j.omtm.2019.09.006>

Yamamoto, S., Nakanishi, K., & Matsuno, R. (1988). *Ion-exchange chromatography of proteins* : CRC Press.

Yamamoto, S., Nakanishi, K., Matsuno, R., & Kamikubo, T. (1983a). Ion exchange chromatography of proteins—prediction of elution curves and operating conditions. I. Theoretical considerations. *Biotechnology and bioengineering*, *25* (6), 1465-1483. doi:<https://doi.org/10.1002/bit.260250605>

Yamamoto, S., Nakanishi, K., Matsuno, R., & Kamikubo, T. (1983b). Ion exchange chromatography of proteins—prediction of elution curves and operating conditions. II. Experimental verification. *Biotechnology and bioengineering*, *25* (5), 1373-1391. doi:<https://doi.org/10.1002/bit.260250516>

Zhao, M., Vandersluis, M., Stout, J., Haupt, U., Sanders, M., & Jacquemart, R. (2019). Affinity chromatography for vaccines manufacturing: Finally ready for prime time? *J Vaccines*, *37* (36), 5491-5503. doi:<https://doi.org/10.1016/j.vaccine.2018.02.090>

#### Figure captions:

**Fig. 1** . Investigated downstream procedure. Suitability of anion-exchange (Q-Sepharose XL) followed by size exclusion Superdex 200 prep grade (pg) for capturing and polishing step. Q-Sepharose XL was fed with 20 fold concentrate of primary feed stock obtained from tangential flow filtration. A final concentration step was included after polishing step for decrease purified sample volume. Then Tris-HCl buffer was replaced by phosphate buffer through diafiltration (DF) before inactivation and formulation.

**Fig. 2** . Elution profile of FMDV from 400x16 mm, I.D. column of Q-sepharose XL (A). Crude FMDV was loaded after dilution with initial buffer, Tris-HCl (20 mM, pH 7.3) and then eluted with elution buffer, Tris-HCl (20 mM, pH 7.3 containing 500 mM KCl). Separation conditions were set as follows: volume of injection: 50 mL, dilution factor: 6, flow rate for sample loading: 3 mL/min, flow rate for elution step: 8 mL/min. Pooled virus fraction was collected from first dimension and applied to the 600x26 mm, I.D. column of Sup-200 stationary phase in the second dimension (B). Separation conditions were set as follows: mobile phase composed 20 mM Tris-HCl (150 mM NaCl, pH 7.3), flow rate 2.5 mL/min and injection volume 4 mL. Chromatograms in both dimension were recorded at 280 nm.

**Fig. 3** . Elution profile of FMDV from 400x16 mm, I.D. column of Q-Sepharose XL (A). Crude FMDV was loaded after dilution with initial buffer, Tris-HCl (20 mM, pH 7.3) and then eluted with elution buffer, Tris-HCl (20 mM, pH 7.3 containing 500 mM KCl). Separation conditions were set as follows: volume of injection: 100 mL, dilution factor: 6, flow rate for sample loading: 3 mL/min, flow rate for elution step: 8 mL/min. Pooled virus fraction was collected from first dimension and applied to the 600x26 mm, I.D. column of Sup-200 stationary phase in the second dimension (B). Separation conditions were set as follows: mobile phase composed 20 mM Tris-HCl (150 mM NaCl, pH 7.3), flow rate 2.5 mL/min and injection volume 4 mL. Chromatograms in both dimension were recorded in 280 nm.

**Fig. 4**. Application HP-SEC on Ultrahydrogel Linear (300 x 7.8 mm, I.D.) analytical column for evaluation fingerprint elution profile during three stage purification strategy. Solid line (Primary crude sample), Dash line (Intermediate concentration step), Dotted line (Second dimension). HP-SEC was performed as follows:

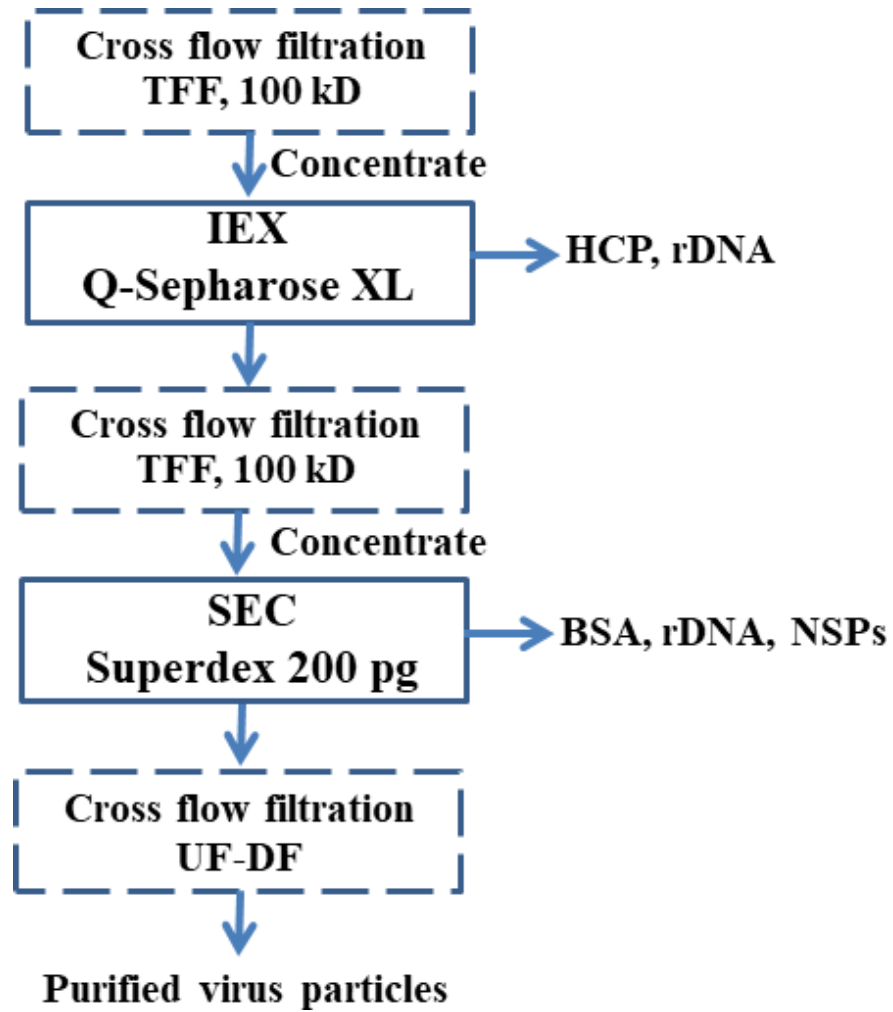
mobile phase; 0.1 M Na<sub>2</sub>SO<sub>4</sub> in 50 mM PBS (pH7.0), injection volume: 50 µl, flow-rate, 0.6 mL/min and detection wavelength: 280 nm.

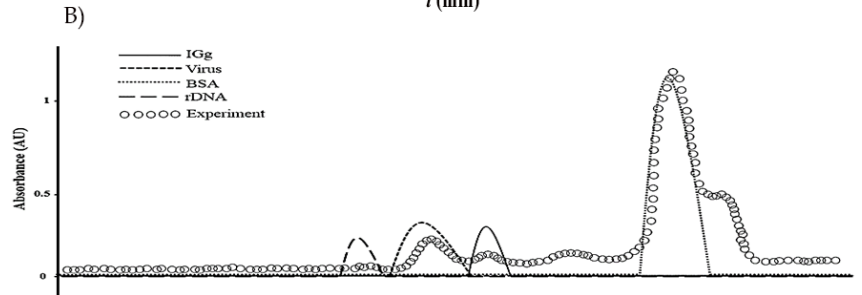
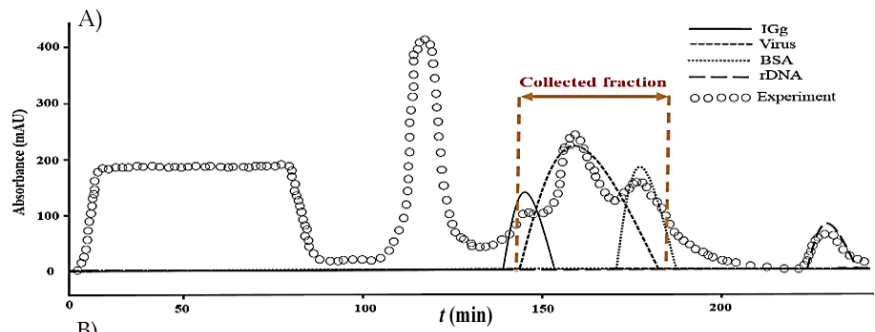
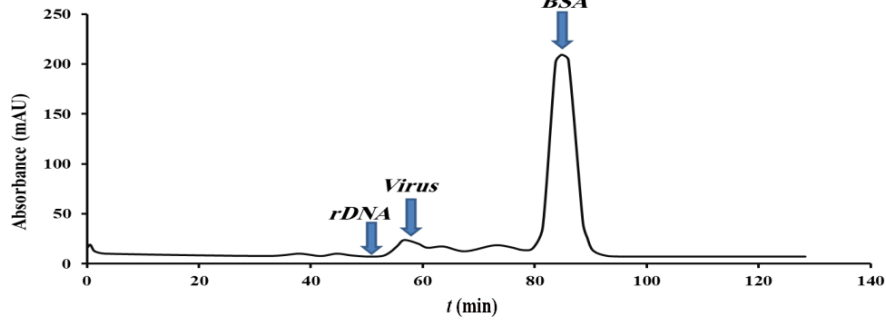
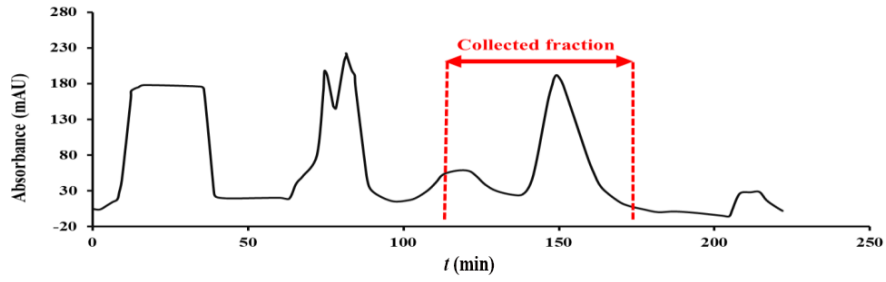
**Fig. 5.** SDS-PAGE of purified FMDV vaccine. Lane 1, Protein markers; Lane 2, 2D-AEC×SEC purified FMDV. The identity of the final product from 2D-AEC×SEC was confirmed by presence of VP1-3 in 20-35 kD and VP4 in 10 kD.

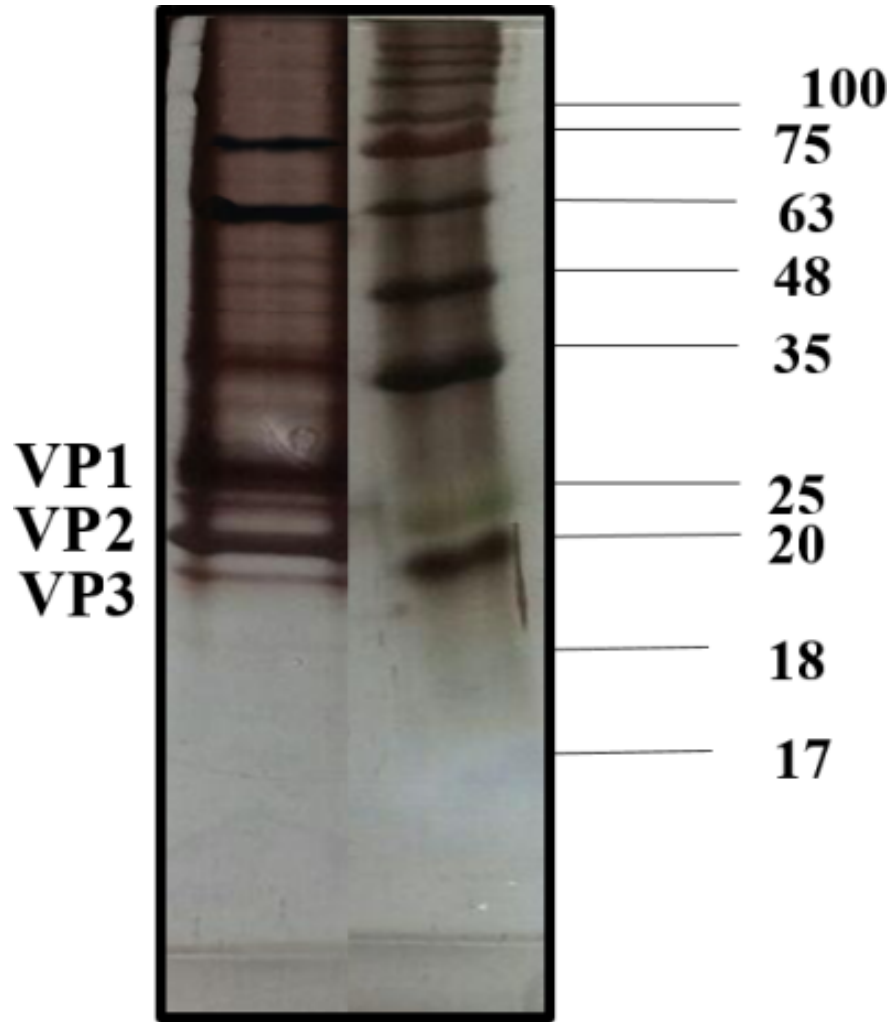
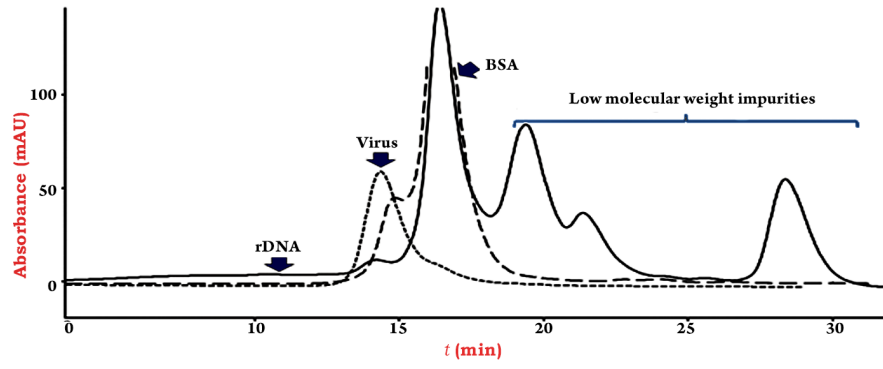
**Fig 6.** MALDI-TOF-MS profiles of purified FMDV particles by 2D-AEC×SEC in low molecular weight 2–20 kD (**A**), medium molecular weight 20–50 kD (**B**) and high molecular weight 50-100 kD (**C**).

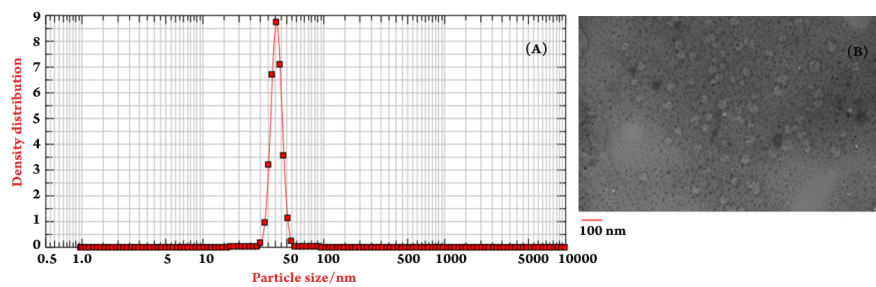
**Fig 7.** Characterization of purified FMDV particles by (A) DLS analysis and (B) TEM imaging.

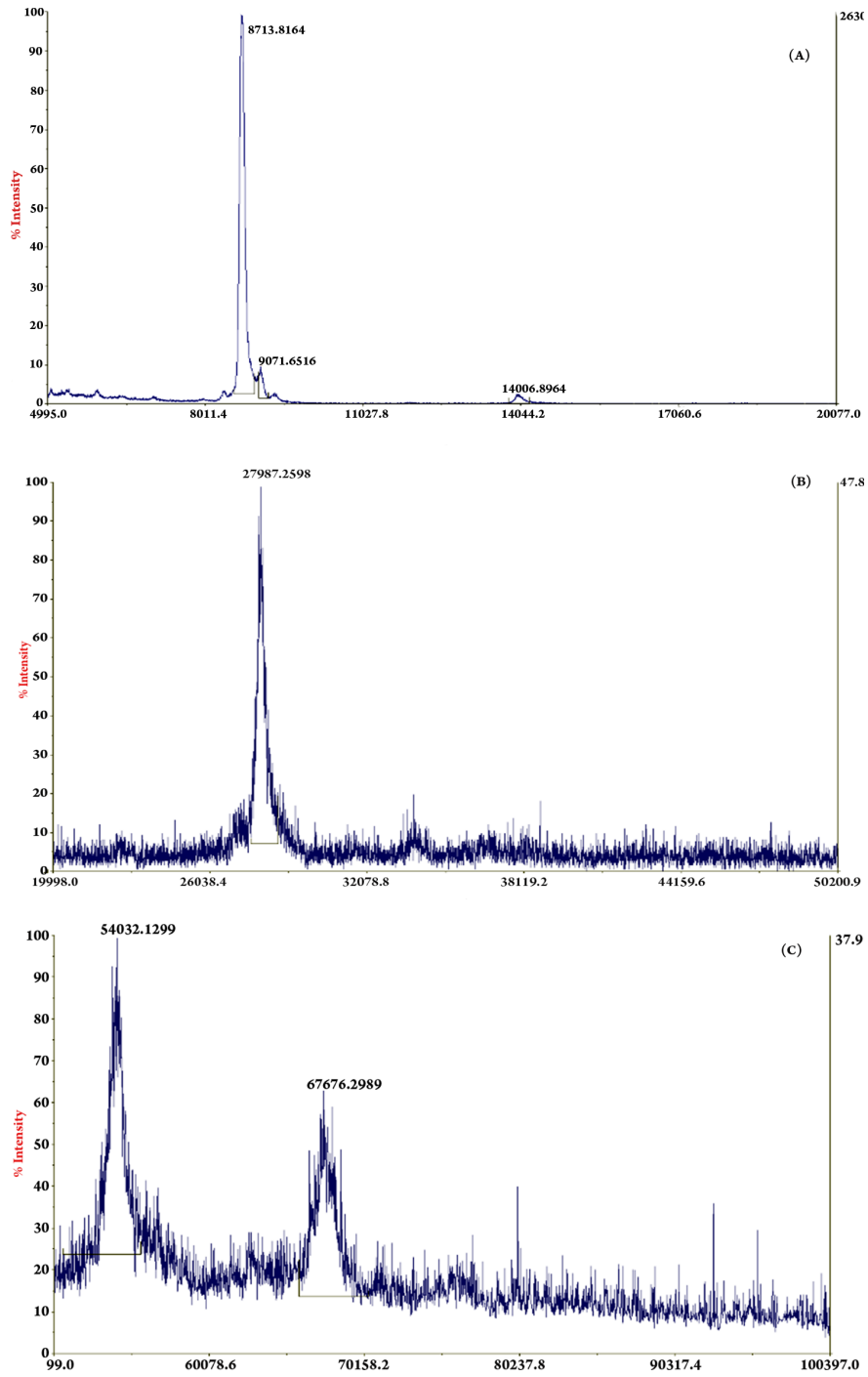
| Table 1.<br>Performance of<br>2D-AEC×SEC<br>for production<br>NSP free FMDV<br>vaccine |
|--|--|--|--|--|
| Sample   | <b>Total Protein<br/>(mg)</b>  | <b>FMDV<br/>Amount (µg)</b>  | <b>FMDV<br/>Recovery (%)</b>   | <b>Residual host cell<br/>DNA (ng)</b>   |
| FMDV crude   | 14.60  | 104.72   | 100.00   | 81.30  |
| First dimension  | 12.50  | 94.02  | 89.80  | 6.80   |
| Intermediate<br>concentration step   | 11.30  | 88.47  | 94.09  | 5.11   |
| Second dimension   | 0.13   | 81.59  | 92.20  | 8.01   |











### Hosted file

Table 1.docx available at <https://authorea.com/users/358187/articles/480441-two-dimensional-anion-exchange-coupling-size-exclusion-chromatography-combined-with-mathematical-modeling-for-downstream-processing-of-foot-and-mouth-diseases-vaccine>

